Available online at www.sciencedirect.com
ScienceDirect
Catalysis Today 133–135 (2008) 49–55
CATALYSIS TODAY
www.elsevier.com/locate/cattod

Transition metals as dopants on nickel borides: Their catalytic activity effect on hydrogenation reactions

Delicia Acosta *, Norma Ramírez, Eleonora Erdmann, Hugo Destéfanis, Elio Gonzo

Instituto de Investigaciones para la Industria Química (INIQUI-CONICET), Facultad de Ingeniería (CIUNSa), Universidad Nacional de Salta (UNSa), Buenos Aires, 177-4400 Salta, Argentina

Available online 19 February 2008

Abstract

Nickel borides doped with elements of first transition series (Cr, Mn, Fe, Co, Cu, and Zn) MNiB, 4% (w/w) respect to Ni, and prepared with the same method as NiB, were used in the glucose and the nitrobenzene hydrogenation reactions. The amorphous catalysts were prepared by chemical reduction of nickel and metallic (Cr, Mn, Fe, Co, Cu, and Zn) salts with borane–tetrahydrofurane (BH_3–THF) complex in aprotic solvent (THF anhydrous). Different techniques were used to characterize these materials. The MNiB amorphous structure was verified by XRD. The results show that bimetallic borides follow a pattern related to the nature of the dopants metal. The oxidation stability, magnetic susceptibility and catalytic effect are correlated with parameters of each dopants metal. SEM studies show the same spongy-morphology in all cases. The logarithm of the ratio between bimetallic boride and nickel borides specific rates, for nitrobenzene hydrogenation, follow a linear relation with respect to the same relation for glucose hydrogenation. These results demonstrate that the dopants effect on the free activation energy is the same for both reaction systems. This effect could be related with electronic modifications introduced by the dopants metal on nickel boride.

Keywords: Nickel borides; Catalyst; Glucose; Nitrobenzene hydrogenation

1. Introduction

It has been known for a long time that it is possible to precipitate black amorphous solids from solutions containing nickel by adding sodium or lithium borohydride [1,2]. These precipitates are considered to exhibit catalytic activity in all kinds of reduction reactions [3,4]. Although their composition remained unclear for 40 years, their annealing behavior was investigated and found to lead to crystalline Ni_2B [5] or Ni_3B [6] and elemental nickel at temperatures near 773 K. The synthesis reaction mechanism has been claimed to include NiX_2 (X = –Cl, $–CH_3COO$) and $LiBH_4$ or $NaBH_4$ as starting materials, and Ni_2B, NaX, hydrogen, and H_3BO_3 as primary products [2], while water, methanol or tetrahydrofurane were the solvents used. Similar procedure is applied when the synthesis of finely divided metals actually is attempted.

It is quite common to synthesize metal borides at temperatures around 1273 K (see for example the synthesis at 1273 K for Ni_3B, at 1473 K for Ni_2B, or 1050–1173 K for Ni_4B_3 [7]), but almost unknown to form a metal boride at temperatures below 573 K. It may well be expected that during the low-temperature synthesis nothing but elemental metal is obtained as a primary product. Boride formation might be suspected to take place when the primary precipitate is annealed at higher temperatures.

On the other hand, nickel borides show to be an alternative way of main importance in hydrogenation processes, especially in selective hydrogenation reactions. The addition of small quantities of a transition metal modifies its activity as well its selectivity in hydrogenation reactions. Recently, amorphous catalysts such as metal-metalloid have increased the interest due to its excellent activity and selectivity and also because for its great resistance to the poisoning with sulfur in different hydrogenation reactions. Amorphous catalysts such as nickel borides were the most studied for the hydrogenation of olefins [8]. The catalytic activity of the nickel boride and nickel Raney [8] could be modified introducing one or more metals in some

* Corresponding author.
E-mail address: acostad@unsa.edu.ar (D. Acosta).

0920-5861/$ – see front matter © 2007 Elsevier B.V. All rights reserved.
doi:10.1016/j.cattod.2007.12.125

steps of the preparation [9,10]. Although considering these interesting perspectives and the possibility to produce changes in the composition of the Ni-borides prepared with our previously reported method [11], there is not a systematic study about the effect produce by the incorporation of a second metal on the rate of reaction. Our work aims to bring more light on the effect produced by dopants metals on nickel borides. We report on its synthesis and characterization via X-ray diffraction, scanning electron microscopy (SEM), infrared FTIR, thermal analysis (TGA/DTA) and chemical composition analysis. In addition, a comparative study of nickel borides doped with transition metals of the first series on glucose and nitrobenzene hydrogenation reactions are presented.

2. Experimental

2.1. Catalyst preparation

Nickel boride (NiB) and nickel metal dopants boride (MNiB) amorphous catalysts were prepared following a previously reported technique [11]. A reducing solution corresponding to the complex diborane–tetrahydrofurane (BH_3–THF) was obtained by reacting 1 g of $NaBH_4$ (Aldrich, 99+%) with 1 ml of H_2O in 100 ml of THF (Mallinckrodt) at 25 °C. This solution was used to reduce the metallic salts. Well-mixed $Ni(CH_3CO_2)_2{\cdot}4H_2O$ (Fluka, 99+) with $Cr_3(CH_3CO_2)_7{\cdot}(OH)_2$ (Aldrich), or $MnCl_2{\cdot}4H_2O$ (Cicarelli, 99+), or $FeCl_3{\cdot}6H_2O$ (Anhedra), or $Co(CH_3CO_2)_2{\cdot}4H_2O$ (Mallinckrodt), or $Cu(CH_3CO_2)_2{\cdot}H_2O$ (Merck), or $Zn(CH_3CO_2)_2{\cdot}H_2O$ (Mallinckrodt) in methanol solution, in necessary quantities to obtain 4% (w/w) proportions of dopants metal over nickel, were added drop wise over BH_3–THF solution with vigorous stirring. All the black powder material obtained by this way was used ''as-prepared'' in catalytic tests.

For characterization purposes the black precipitate was filtered immediately and washed with several amounts of water and THF to remove sodium acetate (a by-product) and unreacted sodium borohydride and finally dried in vacuum at 323 K.

2.2. Characterization

The contents of dopants metals and nickel in metal nickel borides were analyzed by atomic absorption spectroscopy in a GBC 904 AA. Boron contents were simultaneously analyzed as boric acid and by Azometin H molecular absorption technique. The surface area was measured by N_2 adsorption at 77 K in a Micromeritic Flow Sorb Model 2-2300. X-ray diffraction pattern was obtained on a Rigaku D max-IIC with Cu Kα radiation ($V = 40$ kV, $I = 20$ mA) and Ni filter at a scanning rate of 2°/min. Part of the sample was annealed at 500 °C under N_2 flow during 3 h. Thermogravimetric (TG) and DTA studies were carried out in a Rigaku unit at heating rate of 10 °C/min in air. The surface morphology was observed by scanning electron microscopy (SEM; JEOL-JSM-15610LV at 10 kV). FTIR studies were carried out in a Bruker IFS 88B on samples dispersed in KBr. Infrared spectra was recorded ranging 400–800 cm^{-1}. Volumetric magnetic susceptibility for promoted and unpromoted powdered catalyst was measured using a Gouy Balance at room temperature. Experimental data of volumetric magnetic susceptibility are obtained measuring the resultant magnetic force that acts when a powder sample is placed in a known magnetic field. The analytical balance has sensibility of 50×10^{-7} N.

2.3. Hydrogenation conditions

2.3.1. Glucose test

Liquid phase hydrogenation of glucose was performed at 343 K and 5.0 MPa in a stainless steel batch reactor, which contained 2.0 g of fresh catalyst and 0.250 L of glucose aqueous solution. During the hydrogenation, the reaction mixture was stirred vigorously at 1000 rpm to eliminate transport effects [12]. D-(+)-Glucose (Merck) (0.5 M) aqueous solution at pH 6 was used in all cases. A 3 wt% Ni/glucose solution ratio was used. The experiments were carried out under identical conditions to those reported by Acosta et al. [12]. Glucose consumption was followed by a colorimetric method using a specific enzymatic test.

2.3.2. Nitrobenzene test

The liquid phase nitrobenzene hydrogenation was carried out in a shaker Parr 3911 Model reactor under constant total pressure. Fresh catalyst samples, not dried, were used. Nitrobenzene (Mallinckrodt) 1 M in methanol and catalyst concentration of nickel 0.1 mol/L was used in a 0.250 L of mixed solution.

The air in the reaction systems was removed, prior to reaction, using hydrogen at room temperature. In all cases the system was heated up to reaction temperature and then pressurized.

3. Results and discussion

3.1. Preparation and composition analysis

All the samples were prepared following the same methodology using the reducing complex agent. The reducing solution corresponding to the complex tetrahydrofurane–diborane (THF –BH_3) was obtained from $NaBH_4$ with water in stoichiometry quantities in tetrahydrofurane medium, according to the following reaction scheme:

$$BH_4Na(c) + H_2O \Leftrightarrow BH_3(g) + H_2(g) + NaOH(s) \quad (1)$$

$$BH_3(g) + THF(l) \Leftrightarrow THF : BH_3(l) \quad (2)$$

The formation and stabilization of BH_3–THF was demonstrated by Hopps [13] and Brown [14]. This complex allows to reduce [11] nickel and dopants metal salts. The black precipitate obtained from the reaction mixture was filtered immediately and washed with small amounts of water and methanol to remove sodium acetate and unreacted $NaBH_4$, in order to analyze their composition. The chemical analysis show that bulk composition were in all cases formulated as $(M + Ni)B_6$. It isfound that dopants metal loading were the same than the theoretical value (3.8–4%, w/w) for Cr, Co, Cu, Fe, Mn and Zn.

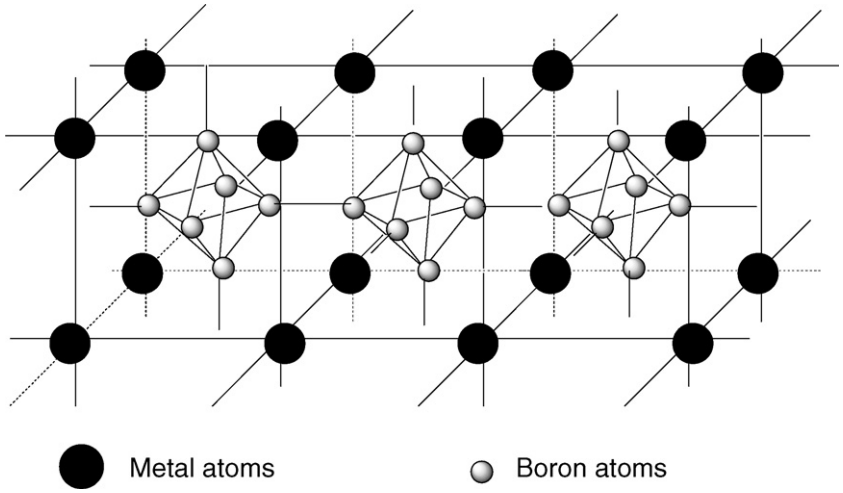

Fig. 1. Structure of metal boride MB6.

According to Shveikin and Cotton [15,16] borides with composition MB_6 (M = metals) is known to form predominant structures where boron atoms can be both, surrounded by metallic centers and forming three-dimensional structure, as shown in Fig. 1. This structure is similar to the body centered cubic in CsCl [16], in which chloride ions has been replaced by octahedral boron (B_6). This octahedral boron is strongly bonded to the edges of the cube and result in an infinite three-dimensional net (Fig. 2).

3.2. TG and DTA analysis

Studies of TG–DTA were carried out at atmospheric pressure. For all samples DTA/TG results exhibit thermal effects between 400 and 500 K as well as in the 800–1100 K range. The thermogravimetric analysis of doped and non-doped nickel borides shows the loss of weight by the elimination of THF and methanol solvents through an endothermic process that occurs at about 473 K. In the temperature range of 973–1083 K a single exothermic peak appears, due to the formation of metal borate by the presence of air in the thermogravimetric experience. This effect was corroborated by XRD and FTIR. The results obtained with NiB are shown in Fig. 3. The difference found between DTA results obtained over doped and non-doped borides is the temperature of the exothermic process. The temperature of the oxidation peak is modified according to the dopant metal (Table 1). As it can be seen, the metal borate phase seems to be more stable when chromium was used.

3.3. Scanning electron microscopy

The electronic microscopy SEM results of doped and non-doped nickel boride are shown in Figs. 4–6. The sponge-like morphology of all the samples could be attributed to the high hydrogen production during its preparation. It could be a consequence of metallic ion reduction reaction by the

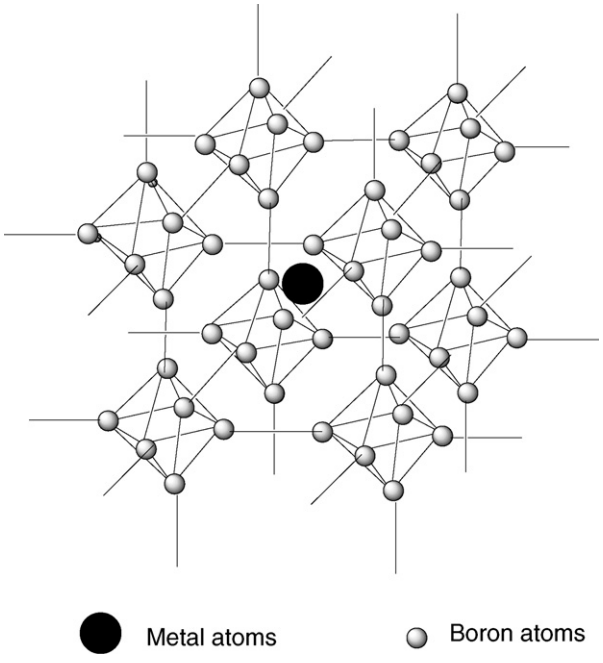

Fig. 2. Structure of metal boron in MB_6.

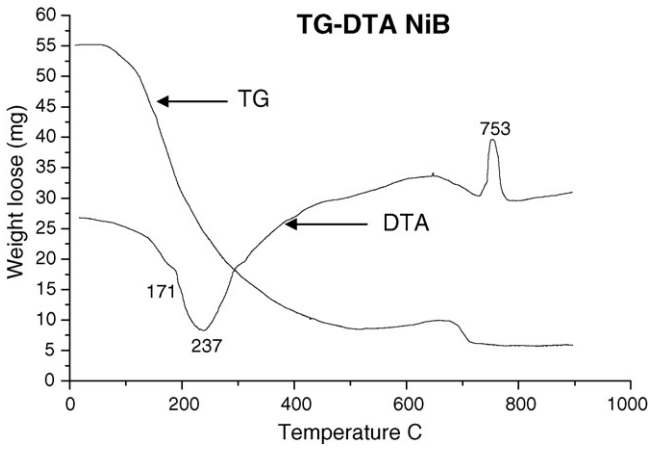

Fig. 3. TG–DTA of non-doped nickel boride.

Table 1
TG and DTA results for nickel boride (NiB) and metallic nickel boride (MNiB)

Nickel boride	Exothermic peak (K)
NiB	949
ZnNiB	974
CuNiB	1006
FeNiB	1018
MnNiB	1031
CoNiB	1048
CrNiB	1081

THF–BH_3 complex that produces metal borides. This was also observed by Xie et al. [17], comparing the surface topology of Ni^{2+} over the silica, after the addition of BH_4^- to obtain NiB. We agree with Xie et al. [17], who considered that the spongy aspect is due to the fact that the solid is constituted by thousands of very tiny particles with an average size around 300 nm. Also, Kapfenberger et al. [18] observed in SEM micrographs the presence of nanometric characteristic particles, with narrow size distribution and diameter about 50 nm. The micrographs also show light colored particles corresponding to the starting oxidation process that appears when the dry sample is exposed to air. This is confirmed by FTIR and XRD after sample calcinations at 1073 K. Moreover, in XRD profiles of borate phases (predominant species) that belong to nickel boride, nickel oxide and metallic nickel (in minor quantities) are obtained (see Fig. 7).

The FTIR studies on the same samples show, as in XRD, borates and NiO characteristic vibration bands. The vibration stretching band of B–O at 1350 cm^{-1} is followed by an asymmetric vibration B–O–B at 1375 cm^{-1} which is confirmed with the symmetric stretching B–O–B at 1260 cm^{-1}. The absorption band at 1500 cm^{-1} could be attributed to the NiB because it does not belong to nickel oxide or borate.

3.4. X-ray diffraction

X-ray diffraction studies performed on the catalyst before and after the catalytic test show amorphous structures as can be seen in Fig. 8. Only one broad peak around $2\theta = 45^\circ$ was observed for the fresh sample indicating a typical amorphous character [17]. In comparison with the fresh sample, a structure change of the catalyst after 30 h reaction test is observed (Fig. 8b). It means that the amorphous structure was destroyed in some extent after being used in catalytic test. The NiB profile after the catalytic test is consistent with the structure of mixtures of NiB and Ni, according to Kapfenberger et al. [18]. However most of the material remains amorphous.

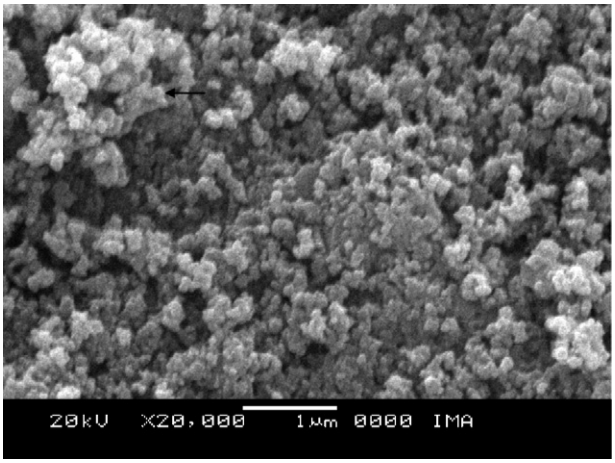

Fig. 5. SEM micrograph of chromium nickel boride.

3.4.1. Thermal treatment

Thermal treatment of doped and non-doped nickel borides samples were carried out to study the phase's transformation. The heating rate was 2 °C/min up to 773 K in N_2 atmosphere. With the increase of treating temperature the broad peak around $2\theta = 45^\circ$ became sharper and several other crystallite diffraction peaks corresponding to metallic nickel appear indicating the occurrence of crystallization processes accompanying decomposition of Ni–B alloy (see Fig. 9). During washing procedure NiO phase appears due to surface oxidation process. As well as in SEM analysis the proportion of NiO and Ni° phases depends upon dopant metal.

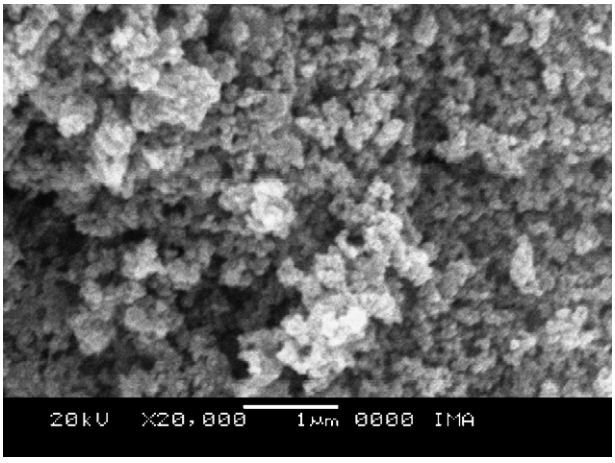

Fig. 4. SEM micrograph of nickel boride.

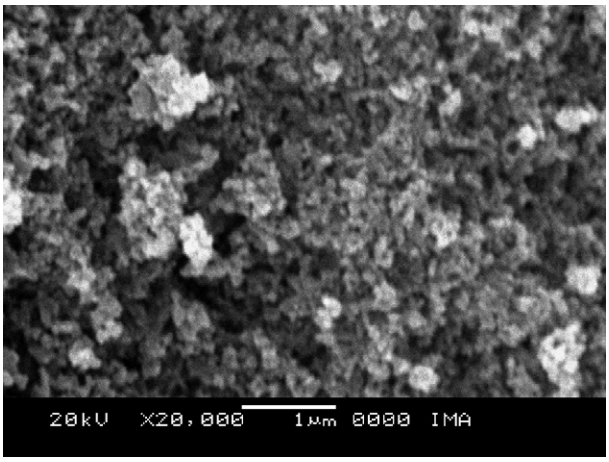

Fig. 6. SEM micrograph of zinc nickel boride.

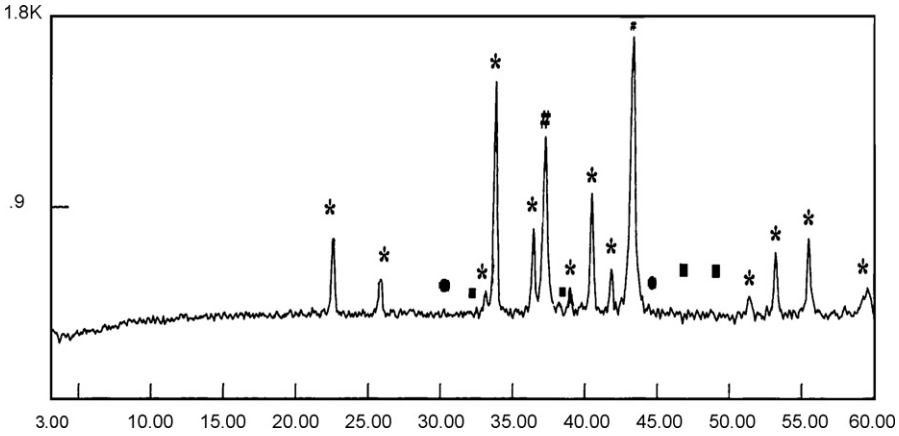

Fig. 7. XRD of NiB annealed to 1073 K. *, phase of $Ni_3(BO_3)_2$ (JCPDS 261284); #, phase of NiO (JCPDS 40835); ●, phase of NiB (JCPDS 60567); ■, phase of Ni (JCPDS 40850).

3.5. Magnetic susceptibility analysis

As can be seen in Fig. 10, CrNiB has the highest magnetic saturation (magnetic susceptibility), even higher than NiB. The magnetization [19] could be attributed to the positive holes in d-band of Ni and the magnetic moment is a measure of the occupancy of this holes. The electronic band theory of metals was applied [20] to explain the chemisorptions changes and the catalytic activity of the alloys with transition metals. Changes in the composition of these alloys modify the energy density of electrons at the Fermi level. For this study the NiB and the bimetallic borides (MNiB) could be classified by the relation boron–metal in the metallic borides where the B forms a net of B–B bonds which gives place to a net produced by metal–metal bonds (Figs. 1 and 2). In this kind of boride the interactions boron–metal are weak, so the metallic net could be considered as an independent alloy of B. Therefore, the effect on the catalytic activity related to the metallic net composition can be analyzed.

The Fermi level of Ni falls slightly below the 3d-band and the magnetism is a consequence of the unpaired moment spin of about 0.6 holes per atom in the d-band. The magnetic moment of Ni in the NiB is almost due to the unpaired spins of the electrons. The magnetization intensity in Bohr magnetrons is practically equal to the number of holes in the d-band. With 0.6 vacancies per Ni atom in the d-band and a contribution of N electrons per atom of the added dopants, the number of holes (n_h) could be calculated with the following equation [20]:

$$n_h = \frac{0.6 - x\,\Delta N}{1 + x} \tag{3}$$

where ΔN = (number of Ni electrons − number of dopants metal electrons) and x is the number of dopants metal atoms per Ni atom. Fig. 10 shows the relationship between magnetic susceptibility and the number of vacancies related to the number of electrons "s + d" and the content of the dopants metal. As can be noticed, a linear relationship is found.

3.6. Activity test for hydrogenation reactions

Preliminary rate measurements were performed on the fresh non-doped catalyst. The dependence of rate upon the stirring speed was previously reported [12] which revealed that there was a plateau above 800 rpm where the rate did not depend on stirring speed. Therefore a standard stirring speed of 1000 rpm was used subsequently. At such stirring speed the rate of glucose hydrogenation shows, in all cases, first order kinetic

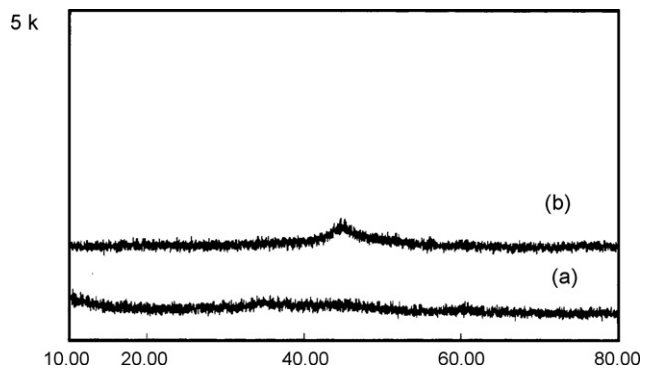

Fig. 8. X-ray diffraction of (a) NiB before catalytic test and (b) NiB after 30 h of catalytic test.

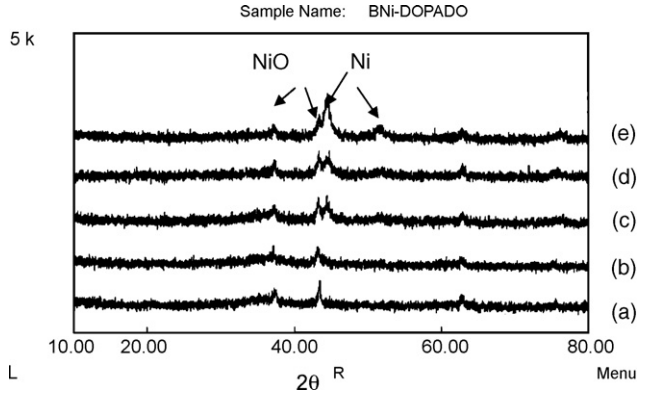

Fig. 9. XRD of nickel metallic dopants borides: (a) ZnNiB, (b) MnNiB, (c) NiB, (d) CoNiB, and (e) CrNiB.

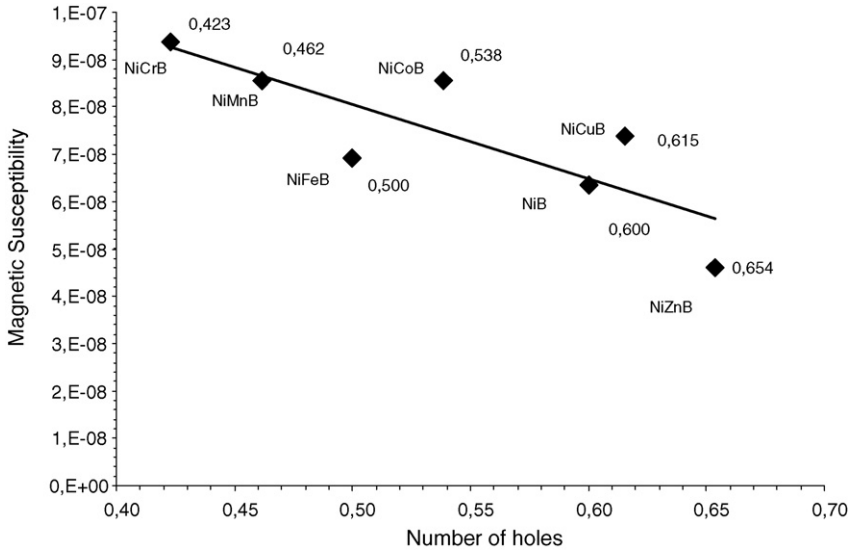

Fig. 10. Magnetic susceptibility of doped and non-doped nickel boride vs. number of holes of dopants metal.

respect hydrogen and zero order respect to the substrate. The same behavior was observed by Li et al. [9].

Nitrobenzene hydrogenation reaction follows a kinetic of first order respect hydrogen and zero order on nitrobenzene concentration, in agreement with data reported by Chen and Chen [21]. The kinetic constant values in the glucose and in the nitrobenzene hydrogenation were obtained by a linear regression of the experimental data. The correlation factor was better than 0.999 in all cases. The experiments were repeated three times in order to achieve statistical value.

Numerous attempts were done to explain the possible role of the dopants metal in the catalytic activity. According to Li et al. [9] and Chen and Chen [21] metal dopants coexist as ions that improve the polarization of the group to be reduced. They established that Cr is present as chromo oxide (III) and Cr^{3+} ions are those that allow the dissociative absorption of the carbonyl group and increase of the catalytic activity. These authors stated that M^{n+} would act as Lewis adsorption sites where a free electronic pair from the carbonyl group adsorbs the glucose molecule. The bond C=O is polarized producing the nucleofilic attack to the atomic hydrogen which was dissociatively chemisorbed on the neighbor Ni.

In our study the preparation method assures, according to TG/DTA, SEM, XRD and chemical composition results, that the added metals were reduced by a reducing agent forming metal–metal bonds. Therefore, the effect produced by the metal dopants cannot be explained through the Hui and Chen postulate [9,21]. Our catalysts belong, according to the boron–metal relationship to a three-dimensional structure. In this kind of structure (Fig. 1), that involves metallic nets, the catalytic activity is a consequence of the changes in the electronic density in the extended orbital of the metal net.

It is well known that, the transition elements series presents monotony in its periodic properties so, a substantial modification in the electron energy could not be inferred, but there are modifications in the electrons population in the Fermi level. This affects the dissociative chemisorptions of hydrogen.

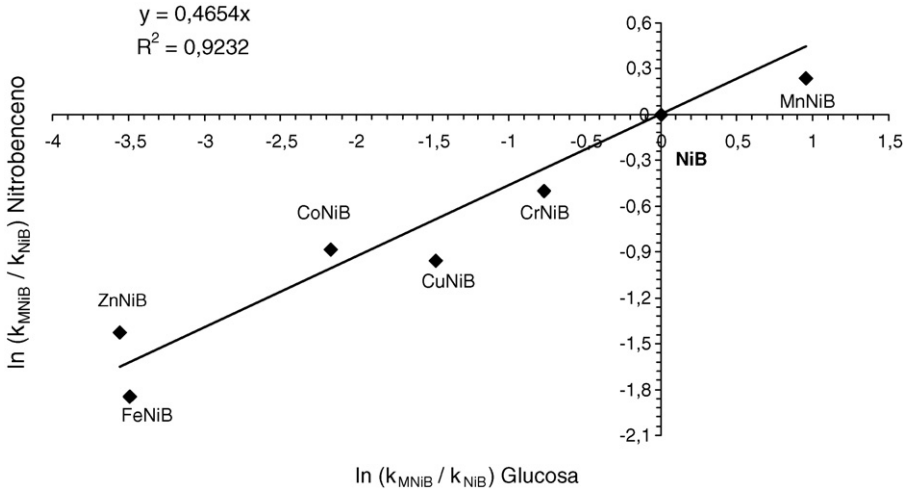

Fig. 11. Specific rate constant for hydrogenation reactions of nickel boride and nickel metallic dopants borides.

The main result obtained is the linear correlation of the logarithm of the ratio between the values of the specific kinetic constants (per unit surface area) of bimetallic borides with that correspondent on pure nickel boride. The straight line in Fig. 11 with a slope ρ is given by

$$\ln \frac{k_{\mathrm{BNiMe}}^{\mathrm{NBenz}}}{k_{\mathrm{BNi}}^{\mathrm{NBenz}}} = \rho \ln \frac{k_{\mathrm{BNiMe}}^{\mathrm{Glucosa}}}{k_{\mathrm{BNi}}^{\mathrm{Glucosa}}} \quad (4)$$

Replacing k as a function of the free activation energy a linear relationship is obtained (Eq. (5)). Therefore, it is clear that the effect produced by the addition of the dopants metal on the controlling step activation free energy is the same for both hydrogenation reactions, which is related to the modification of the electronic energy due to the presence of the dopants metal. The value of the proportionality factor "ρ" is related to the nature of the chemical species in each reacting system.

$$\Delta\Delta G^{\mathrm{NBenz}} = \rho\, \Delta\Delta G^{\mathrm{Glucosa}} \quad (5)$$

4. Conclusions

The results show that all the materials obtained are metallic borides, a unique species such as that seen in the thermal analysis of the samples (TG–DTA). From these results we concluded that the addition of a dopant co-metal modify the stability of this unique species, and consequently its catalytic and magnetic behavior. The SEM micrographs show that the addition of a dopant metal does not produce changes in the surface morphology, but it shows surface oxidation phenomena. This also shows that it is associated to the properties of the co-metals added.

In consequence, depending on the electronic nature of the co-metal added, the properties of the resulting material are modified producing the same effect on the catalytic activity in the glucose and nitrobenzene hydrogenation reactions. It means that the effect on the free activation energy is the same for both reacting systems. This behavior, as well as that observed in the magnetic susceptibility, is consequence of the modification in the electronic population of extended orbital of the metallic net.

Acknowledgements

CONICET and CIUNSa, Research Council of Universidad Nacional de Salta, and Facultad de Ingenieria have supported this work.

References

[1] H.C. Brown, C.A. Brown, J. Am. Chem. Soc. 84 (1962) 1493.
[2] C.A. Brown, J. Org. Chem. 35 (6) (1970) 1900.
[3] C.A. Brown, V.K. Ahuija, J. Org. Chem. 38 (1973) 2226.
[4] K. Molvinger, M. Lopez, J. Court, Tetrahedron Lett. 40 (1999) 8357; K. Molvinger, M. Lopez, J. Court, J. Catal. A: Chem. 150 (1999) 267.
[5] H.I. Schlessinger, H.C. Brown, A.E. Finholt, J.E. Gilbreath, H.R. Hoestra, E.K. Hyde, J. Am. Chem. Soc. 75 (1953) 215.
[6] L.J.E. Hoffer, J. Schultz, R.D. Panson, R.B. Anderson, Inorg. Chem. 3 (1964) 1783.
[7] S. Rundqvist, Acta Chem. Scand. 13 (1959) 1193.
[8] Hamar-Thibault, J. Masson, Vidal, Appl. Catal. A: Gen. 99 (1993) 131–159.
[9] H. Li, H. Li, J.-F. Deng, Catal. Today 74 (2002) 53–63.
[10] B.W. Hoffer, E. Creeza, Devred, Appl. Catal. A: Gen. 253 (2003) 437–452.
[11] H. Destéfanis, D. Acosta, E. Gonzo, Catal. Today 15 (1992) 555–564.
[12] D. Acosta, H. Destéfanis, E. Gonzo, Latin Am. Appl. Res. 24 (1994) 2253–2256.
[13] H. Hopps, Chem. Eng. News 52 (41) (1974) 3 (Aldrich-Borane Inc., USA).
[14] H.C. Brown, J. Am. Chem. Soc. 82 (1960) 4703–4707.
[15] G.P. Shveikin, A.L. Ivanovskii, Russ. Chem. Rev. 63 (9) (1994) 11–734.
[16] F.A. Cotton, G. Wilkinson, Química Inorganica Avanzada, Limusa, Mexico, 1975, pp. 275–278.
[17] S. Xie, H. Li, H. Li, J.-F. Deng, Appl. Catal. A: Gen. (1999) 45–52.
[18] C. Kapfenberger, K. Hofmann, B. Albert, Solid State Sci. 5 (2003) 925–930.
[19] Magnetochemistry, Intersience Pub. Inc., 1956 (Chapter 15).
[20] A. Clark, The Chemisorptive Bond. Basic Concepts, Academic Press, New York & London, 1974, p. 49 (Chapter IV).
[21] Y.Z. Chen, Y.C. Chen, Appl. Catal. A: Gen. 115 (1994) 45–57.